The relationship between the fine structure of amylopectin and the type of crystalline allomorph of starch granules in rice endosperm

Yasunori Nakamura[a,b,*], Kazuki Yashiro[c], Go Matsuba[c], Yifei Wang[d], Goro Mizutani[d], Masami Ono[a], Jinsong Bao[e]

[a] *Starch Technologies Co., Ltd., Akita Prefectural University, Shimoshinjo-Nakano, Akita-city, Akita 010-0195, Japan*

[b] *Faculty of Bioresource Sciences, Akita Prefectural University, Shimoshinjo-Nakano, Akita-city, Akita 010-0195, Japan*

[c] *Graduate School of Organic Materials Engineering, Yamagata University, 4-3-16 Jonan, Yonezawa, Yamagata 992-8510, Japan*

[d] *School of Materials Science, Japan Advanced Institute of Science and Technology, 1-1 Asahidai, Nomi, Ishikawa 923-1292, Japan*

[e] *Institute of Nuclear Agricultural Sciences, Zhejiang University, Hangzhou 310058, China*

*Corresponding author: Starch Technologies Co., Ltd., Akita Prefectural University, Shimoshinjo-Nakano, Akita-city, Akita 010-0195, Japan.

E-mail address: nakayn@silver.plala.or.jp (Yasunori Nakamura)

Abstract

Background and Objectives: It is known that any wild-type varieties of cereals so far examined have A-type starch crystals in their endosperm whereas their *starch branching enzyme 2b* (*be2b)* mutants that are usually referred to as *amylose-extender* (*ae)* mutants produce B-type starch crystals. The present study aimed to examine the structural features of amylopectin which are responsible for the A-type or B-type crystalline allomorphs of starch granules by using starches in wild-type *japonica* and *indica* rice varieties and their *be2b* (*ae*) mutants.

Findings: The average length of chains of A-type amylopectin was markedly shorter than that of B-type amylopectin. It was also thought that A-type amylopectin had two types of branches, namely the first branches were formed mainly by BEI in the basal region of the cluster and the second branches were synthesized specifically by BEIIb inside the cluster. These differences caused the average length of double helices formed by cluster constituent chains to be shorter in wild-types than that in their *be2b* mutants, and these differences changed the crystalline allomorph of starch granules to B-type in the mutants from A-type in their wild-types, as examined by wide angle X-ray diffraction (XRD) and sum frequency generation spectroscopy (SFG).

Conclusions: Combined with these observations and calculations of chain-length of hypothetical A chains in four types of amylopectin molecules, it was concluded that both the average length of external segments of cluster chains and the formation of the second branches inside the cluster greatly affect the crystal types of starch granules.

Significance and Novelty: The novel findings in the present study can provide new insights into the structural features of amylopectin which determines the A-type or B-type crystalline allomorph of starch granules of cereals.

Keywords A-type starch; B-type starch; rice endosperm; starch branching enzyme

Abbreviations *ae*, amylose extender; APTS, 8-amino-1,3,6-pyrenesulfonic acid; BE, starch branching enzyme; DBE, starch debranching enzyme; DP, degree of polymerization; FACE, fluorophore-assisted carbohydrate electrophoresis; Φ-LD, phosphorylase-limit dextrins; PaISA, Isoamylase from *Pseudomonas amyloderamosa*; SFG, sum frequency generation spectroscopy; SS, starch synthase; XRD, wide angle X-ray diffraction

1 INTRODUCTION

Rice plants have been widely used as materials for studies on starch biosynthesis. Rice varieties are largely classified into *japonica*-type and *indica*-type varieties. Past investigations have revealed that starch is synthesized by concerted actions of starch synthase (SS), BE, and starch debranching enzyme (DBE). Although three starch biosynthetic enzymes have multiple isozymes, their roles and expressions in various organs and tissues are greatly different in rice plants (Ohdan et al., 2005). It has been established that *japonica*-type rice is deficient in SSIIa, whereas *indica*-type rice has a full activity of SSIIa (Umemoto et al., 2002; Nakamura et al., 2005).

Starch is composed of amylopectin, a highly branched glucan, and amylose, an essentially linear glucan, and the amount of amylopectin usually accounts for 65-85% of the total starch. Amylopectin is known to have a specific fine structure. This glucan has a structural element called "cluster", which is interconnected by long chains and aligned basically in tandem fashion (French, 1972; Nakamura & Kainuma, 2022). Each cluster is composed of A chains (non-branched chains) and B1 chains (branched by at least one chains) and each cluster is interconnected by long chains designated as B2 chains and/or B3/B4 chains that span to two/three clusters and/or three clusters, respectively (Peat et al., 1952; Hizukuri, 1986). Very importantly, when non-branched segments of neighboring chains of the cluster exceed 10 glucosyl units or degree of polymerization (DP) of 10, they form double helices (Gidley & Bulpin, 1987). The presence of double helices in amylopectin molecules dramatically affects physicochemical properties of starch granules including amylopectin and amylose molecules. The clusters are packed by the lateral alignment of neighboring double helices (Kainuma & French, 1972; Yamaguchi et al., 1979; French, 1984). It is widely known that starch granules in cereal endosperm show the A-type crystalline polymorph whereas some tubers and rhizomes exhibit the B-type crystalline polymorph, which can be clearly distinguished by X-ray diffraction analysis (see reviews by Hizukuri, 1996; Buléon et al., 1998). The A-type starch is composed of a monoclinic unit cell whereas the B-type starch has a hexagonal unit cell, and thus the A-type starch is considered to be more densely packed compared with the B-type starch (see review by Imberty et al., 1991).

The phenotypes of BEIIb-deficient mutants of cereals are often designated as *ae* because the *ae* mutant starches have apparently the high-amylose contents in the endosperm (see review by Shannon et al., 2009). Interestingly, the *ae* starches in cereal endosperm show the B-type crystalline allomorph (Gérard et al., 2000; Nishi et al., 2001; Tanaka et al.,

2004). The *be2b* (*ae*) mutants in *japonica*-type rice endosperm (Yano et al., 1985) have a modified amylopectin chain profile because it contains more long B chains and fewer short chains of DP ≤ ca. 13 (Nishi et al., 2001; Nakamura et al., 2022). This change is caused by loss of the distinct role of BEIIb, playing an essential role in the synthesis of short chains in the region in the crystalline lamella of amylopectin cluster (Jane et al., 1997; Nakamura et al., 2020). Based on these observations, recently we proposed that amylopectin in endosperm of *japonica*-type rice and its *be2b* mutant is referred to as A-type amylopectin and B-type amylopectin, respectively (Nakamura et al., 2022). On the other hand, *indica*-type amylopectin has fewer short chains of DP ≤ 10 and more intermediate chains of DP 12-24 than *japonica*-type amylopectin whereas the proportion of long chains is unchanged between these amylopectin (Umemoto et al., 1999; Nakamura et al., 2002). However, *indica*-type starch granules exhibit A-type allomorph as *japonica*-type starch granules (Hizukuri, 1996). In this sense, *indica*-type amylopectin should be classified into an A-type amylopectin.

What is a criterion to distinguish the structural difference between A-type and B-type amylopectin? In the present study, to analyze the structural difference between A-type amylopectin and B-type amylopectin, the fine structure of endosperm amylopectin of *be2b* (*ae*) mutants from both *japonica* rice and *indica* rice was analyzed in details, because both *be2b* mutant starch granules would have B-type crystalline allomorph, whereas the A-type amylopectin structure is known to be greatly different between *japonica* and *indica* rice varieties. Therefore, these materials used in this study are extremely beneficial to reveal the relationship between the fine structure of amylopectin and the crystalline allomorph of starch granules. In addition, to analyze the internal structure of amylopectin, chain-length distribution of its phosphorylase-limit dextrin (Φ-LD) was examined. To reveal the relationship between the fine structure of amylopectin and the internal starch structure of starch granule, starch crystalline structures were also examined using XRD and SFG analysis (Miyauchi et al., 2006; Kong et al., 2014).

2 MATERIALS AND METHODS

2.1 Reagents

A fluorophore 8-amino-1,3,6-pyrenesulfonic acid (APTS) was obtained from AB SCIEX (Tokyo, Japan). α-Glucan phosphorylase from rabbit muscle was purchased from SIGMA.

Isoamylase from *Pseudomonas amyloderamosa* (PaISA) was kindly provided from Hayashibara Co., Ltd., Japan.

2.2 Plant materials and sampling

Two *be2b* mutant lines EM10 and IR36*ae* were generated from a *japonica*-type cultivar Kinmaze and an *indica*-type cultivar IR36, respectively. Mature seeds were also harvested from each line which was grown in the experimental field of Akita Prefectural University under natural environmental conditions during summer months, and stored at 8°C before use.

2.3 Preparation of starch granules from rice endosperm

Starch granules from randomly chosen mature endosperms of each line were prepared as described previously (Nakamura et al., 2020).

2.4 Chain-length distribution analysis of amylopectin

The chain-length distribution of amylopectin was analyzed by using the fluorophore-assisted carbohydrate electrophoresis (FACE) method (O'Shea et al., 1998) after treatment of amylopectin with PaISA to remove α-1, 6-glucosidic linkages, followed by labelling of APTS at the reducing ends of debranched glucan chains, as described previously (Nakamura et al., 2020).

2.5 Chain-length distribution analysis of phosphorylase-limit dextrins (Φ-LD) of amylopectin

Chain-length distribution of Φ-LD was analyzed to examine the internal structure of amylopectin. In this analysis, amylopectin was treated with a rabbit muscle phosphorylase to form its Φ-LD, as reported previously (Sawada et al., 2014). The Φ-LD was debranched and its chain-length distribution was analyzed as above.

2.6 X-ray diffraction (XRD) pattern analysis of starch granules

XRD measurements were performed on a Nano-viewer system (Rigaku Co., Tokyo, Japan) at a wavelength of 0.154 nm (CuKα). The camera lengths were 75 mm. A Pilatus

1M (Dectris AG, Baden, Switzerland) detector was used, with a q range of 3.5 to 25 nm^{-1}; q is the magnitude of the scattering vector and is defined as follows:

$q = 4\pi \sin\theta \ /\lambda$ (1),

where 2θ and λ are the scattering angle and wavelength, respectively. The starch granule samples were put into the sample cell of approximately 500 μm thickness. Data processing, which included controlling the contrast of the 2D-patterns and the preparation of a 1D-profile from the obtained 2D-patterns, was performed using the FIT-2D software (Ver. 12.077, Andy Hammersley/ESRF, Grenoble, France).

2.7 Optical sum frequency generation (SFG) spectroscopy of starch granules

The powdered starch samples of Kinmaze, IR36, EM10, and IR36*ae* were put in transparent silica glass square cells (AS ONE Q-101; 3.5 mm × 12.5 mm × 45 mm). The internal sizes of the cells were 1 mm in thickness and 10 mm in width. SFG of our sample was observed through the glass window of the cell. The SFG spectroscopy system was the same as previously described (Hieu et al., 2015; Nakamura et al., 2020). Tunable infrared light pulses at wavelength of approximately 3 μm was output from an optical parametric generator (EKSPLA PG401/DFG2-18P) pumped by the fundamental and third harmonic output of a Nd^{3+}:YAG laser (EKAPLA PL2143B) with time width 30 ps and repetition rate of 10 Hz. The pulse energy of the visible light was about 10 μJ and that of the infrared was about 260 μJ at the sample. The spectral width of the IR light was 6 cm^{-1}. For more details see our previous paper (Nakamura et al., 2020).

3 RESULTS

3.1 Comparison of chain-length distribution of amylopectin in mature endosperm of *be2b* mutant lines and their parent cultivars of *japonica*-type rice and *indica*-type rice

It is widely known that starch granules including amylopectin in mature endosperm of wild-type rice from both *japonica*-type and *indica*-type varieties have the A-type crystalline allomorph. We previously proposed that the rice amylopectin structure is referred to as the A-type amylopectin or B-type amylopectin based on the criterion that its starch granules show the A-type or B-type crystalline allomorph, such as wild-type or *be2b* mutants, respectively (Nakamura et al., 2022). To characterize the structural features

of amylopectin, its chain-length distribution from a *japonica*-type line Kinmaze and an *indica*-type line IR36 was measured and compared by the FACE method. Both chain profiles have two major peaks; a large peak consisting of short chains of having DP 6 to approximately 34 (A and B1 chains) and a small peak consisting of long chains having DP ≥ approximately 37 (cluster-interconnecting B2-B4 chains) (Figs. 1A and 1B). Figs. 1C and 1D show that although both of their *be2b* mutant (*ae* mutant) lines EM10 and IR36*ae* also had two major peaks, the proportion of long chains (B2-B4 chains) to short chains (A and B1 chains) was markedly increased by the loss of BEIIb activity (Supplementary Table S1).

Fig. 2 shows the differences in endosperm amylopectin chain-length distribution between *japonica*-type and *indica*-type lines and between wild-type and *ae* type lines. The amylopectin in *japonica*-type *ae* mutant line EM10 had fewer very short chains of DP 6-12 with a peak of DP approximately 8-10 and more long chains of DP ≥ about 37 and intermediate chains of DP 14-30 compared with Kinmaze amylopectin (Fig. 2A). Notably, the similar pattern of differences in chain-length distribution of amylopectin between *indica*-type mutant line IR36*ae* and its wild-type line IR36 was detected, although the extent of differences between *indica*-type lines was significantly lower than that between *japonica*-type lines (Figs. 2A and 2B). The pattern of difference in chain-length distribution of amylopectin between the SSIIa-deficient *japonica*-type rice and the SSIIa-active *indica*-type rice was clearly different from that between the *ae*-mutant and its wild-type (Compare Fig. 2B with Figs. 2A and 2C). The proportion of very short chains of DP 6-10 was higher but that of intermediate chains of DP 13-24 was lower in a *japonica*-type line Kinmaze than an *indica*-type line IR36, whereas there was no significant difference of B2-B4 chains between two lines (Fig. 2B and Supplementary Table S1), consistent with our previous studies (Umemoto et al., 1999; Nakamura et al., 2002, 2005).

3.2 Comparison of chain-length distribution of phosphorylase-limit dextrins (Φ-LD) of amylopectin in mature endosperm of *be2b* mutant lines and their parent cultivars of *japonica*-type rice and *indica*-type rice

To examine the internal structure of amylopectin more in details, the external segments of chains were digested by a rabbit muscle phosphorylase a (SIGMA) and then the chain-length distribution of the resulting Φ-LD was determined by the FACE method. In this analysis, almost all of the chains of DP 4 are considered to be derived from A chains. According to this criterion, the amounts of A chains (DP 4-chains) were approximately

52%, 57%, 52%, and 55% in Kinmaze, EM10, IR36, and IR36ae, respectively (Fig. 3), indicating that the proportion of A chains in amylopectin was significantly higher in either *be2b* mutant than that in its wild-type. Fig. 4 compares the chain profiles of Φ-LD. Compared with wild-type Kinmaze, Φ-LD of its *be2b* mutant EM10 had fewer chains of DP 6-18 and enriched chains of DP 24-37 (Fig. 4A). The result suggests that the wild-type amylopectin had more branches inside the cluster, and therefore some chains carried multiple branched chains. This resulted in longer internal chain-length in Kinmaze amylopectin than EM10 amylopectin. Fig. 4B shows that Φ-LD from *japonica*-type Kinmaze had more A chains but slightly less short internal segments of DP 6-9 than that from *indica*-type IR36. This suggests that the IR36 amylopectin had slightly more B1 chains with short internal segments of DP 6-9 to some extent than the Kinmaze amylopectin. Figure 5 illustrates the structural features of amylopectins of Kinmaze and IR36 and their *ae* mutants, although the difference of amylopectin between EM10 and IR36*ae* was too small to present it in the figure.

3.3 X-ray diffraction (XRD) patterns of starch granules in in mature endosperm of *be2b* mutant lines and their parent cultivars of *japonica*-type rice and *indica*-type rice

Fig. 6 shows the XRD profiles of various starch granules in mature endosperms of Kinmaze, IR36, EM10 and IR36*ae*. The XRD profile of Kinmaze (Fig. 6A) and IR36 (Fig. 6B) had peaks at the scattering vector, *q*, of approximately 10.58 (a single peak), 12.03 and 12.71 (doublet peaks), and 16.18 nm^{-1} (a single peak), which are characteristics of A-type starch granules in cereal endosperm. On the other hand, the XRD profile of EM10 (Fig. 6C) and IR36*ae* (Fig. 6D) had peaks at *q* of approximately 3.724 (a single peak), 11.38 (a single peak), 15.54 and 16.92 nm^{-1} (doublet peaks), which are characteristics of B-type starch granules (Nagasaki et al., 2021; Nakamura et al., 2022).

3.4. Optical sum frequency generation (SFG) spectroscopy of starch granules in mature endosperm of *be2b* mutant lines and their parent cultivars of *japonica*-type rice and *indica*-type rice

Figure 7 shows SFG spectra obtained for starch granules in mature endosperms of Kinmaze, EM10, IR36, and IR36*ae*. The curves represent the SFG intensity fit to Lorentzian curves in Eq. (1) below with fitting parameters in Table S1.

$$|\chi^{SFG}|^2 = \left|\chi^{NR} + \sum_{n=1}^{5} \frac{A_n \exp(i\theta_n)}{\omega - \omega_n + i\gamma_n}\right|^2 \qquad (1)$$

Big peaks at around 2910 cm^{-1} and 2970 cm^{-1} were previously assigned to C-H and C-H_2 stretching vibrations, respectively (Kouyama et al., 2016), but the appearance of the separate peaks around 2870 cm^{-1} suggests that we should reconsider the assignments. For the present we assigned the peaks at 2870 cm^{-1}, 2910 cm^{-1}, and 2960 cm^{-1} as CH or CH_2 vibrations. The broad peak around 3100cm^{-1} was tentatively assigned to H_2O peak in our previous paper (Nakamura et al., 2020).

In our previous paper (Nakamura et al., 2020) we reported that starch from the matured endosperms of Kinmaze and EM10 show different SFG spectra according as they are A- and B-type, respectively (Kong et al., 2014). This difference was reproduced in Fig. 7A (Kinmaze) and 7B (EM10). Figures 7A and 7D, SFG spectra of starch granules in mature endosperms of IR35, an *indica-type* cultivar, and IR36*ae*, a *be2b* mutant line of IR35, had similar shapes to Figs. 7A and 7B, respectively. This tendency was also reflected in the list of resonant frequencies in Supplementary Table S2. Namely, the SFG spectra of Kinmaze and IR36 had three resonant oscillators between 2900 cm^{-1} and 3000 cm^{-1}, while those of EM10 and IR36*ae* have two. Thus, it was confirmed that the effect of BEIIb was clearly correlated with the SFG spectral shapes.

4 DISCUSSION

4.1 The structural features of A-type and B-type amylopectin in rice endosperm

The present paper analyzed the fine structures of A-type and B-type amylopectins that give rise to A-type and B-type crystals, respectively, of starch granules of rice (Figs. 1-4). The results confirmed that both *japonica*-type and *indica*-type amylopectin had two types of branches, while branches of their *be2b* mutant ones were present only in the amorphous lamellae (Fig. 5), consistent with our previous study (Nakamura, 2002, 2015, Nakamura et al., 2005, 2020, 2022). This model well explains the reason why the average length of external segments of cluster chains is longer in the B-type amylopectin in *be2b* mutants than that in the A-type amylopectin in their wild-types.

It is known that BEIIb is specifically expressed in rice endosperm, affecting the structural features of amylopectin and crystalline properties of starch granules (Nishi et al. 2001; Nakamura 2018; Nakamura et al. 2020; Ying et al. 2022). When BEIIb activity was lost in the endosperm, chains of amylopectin became longer (Fig. 2), resulting in formation of longer double helices, and this caused starch granules properties to be resistant to thermal gelatinization and the crystalline allomorphs to change to the B-type

from the A-type, as determined by XRD (Fig. 6) and SFG analyses (Fig. 7), consistent with our recent studies (Nakamura et al., 2020; Ying et al., 2022; Zhang et al., 2022) and past investigations by other groups worldwide (Wei et al., 2010; Butardo et al., 2011).

4.2 Structural boundary between the A-type amylopectin and the B-type amylopectin

Although amylopectin chains from an *indica*-type rice were longer than those from a *japonica*-type amylopectin in wild-type, both starches showed A-type crystalline allomorph (Figs. 6 and 7). The fine structure of amylopectin was very similar between the *be2b* mutants generated from the *japonica*-type line EM10 and the *indica*-type line IR36*ae* (Fig. 2D), and in fact their starch granules exhibited the B-type allomorph (Figs. 6 and 7). However, it is noted that in terms of chain-length profile, the *indica*-type IR36 amylopectin appeared to be more similar to the *be2b* mutant amylopectin compared with the *japonica*-type Kinmaze one (Compare Fig. 2C with Fig. 2A, Supplementary Table S1). The analysis of Φ-LD of amylopectin can give us an invaluable information on the features of amylopectin internal structure as well as the proportion of and chain-length distribution of A-chains. The Φ-LD of the *be2b* mutant amylopectin had depleted short B chains of DP approximately 6-20 and more long B chains of DP about 24-37 compared to wild-type amylopectin (Fig. 4A). The result suggests that B chains of the *be2b* mutant amylopectin had longer internal segments than those of its wild-type amylopectin. This is consistent with an assumption that B1 chains of wild-type amylopectin carry branches inside (the crystalline lamellae) as well as amorphous lamellae of the cluster, whereas B chains of the *be2b* mutant amylopectin have branches almost in the amorphous lamellae, as illustrated in Fig. 5. This idea on the structural change of the cluster in the *ae* mutant is consistent with the cluster structure proposed by Waigh et al., (2000) that the average length of the amylopectin helices is longer in B-type starches compared with that in A-type starches. The proportion of A chains was significantly higher in the *be2b* mutant amylopectin than that in the wild-type amylopectin (Fig. 3 and 4). The results suggest that new branches in the amorphous lamellae were more easily formed in B chains than in A chains compared with those in the crystalline lamellae, because A chains become B chains when they are used as acceptor chains.

Irrespective of phosphorolysis of amylopectin, number of total chains are unchanged. It is also considered that the number of cluster-interconnecting chains is unchanged by the treatment of amylopectin with phosphorylase. Therefore, amylopectin chain length distribution can be extrapolated by adding chain-length of DP 12 to each chain of Φ-LD.

In this way, the hypothetical chain profiles for A chains can be calculated. Fig. 8 compares the chain-length distribution of possible A chains of amylopectin from 4 lines used in this study. If this hypothesis is correct, amylopectins of both wild-types and their *be2b* mutants had A chains of DP approximately 6-18. Although it is known that short chains of DP ≤ 9 are unable to form double helices (Gidley and Bulpin, 1987), the proportion of these short chains in total amylopectin chains were only 15.7, 4.7, 7.8, and 4.7% in Kinmaze, EM10, IR36, and IR36*ae*, respectively (Fig. 8). This shows that most of A chains of amylopectin in these lines participated in the formation of double helices, facilitating crystalline properties of starch granules. However, it is noted that the proportion of these chains of DP 6-9 was greatly lower while the proportion of DP 10-18 chains and in particular, that of DP 17 and 18 chains were significantly higher in the *be2b* (*ae*) mutants than that in wild-types. The results indicate that *be2b* mutant amylopectin had longer double helices than wild-type amylopectin. Therefore, it is concluded that all these structural features of amylopectin determined starch granules to be the A-type or the B-type crystalline allomorph. It is widely known that that the crystal type of starch is largely dependent of length of external segments of amylopectin. Generally, shorter chains favor the formation of A-type allomorph whereas longer chains contribute to the formation of B-type allomorph (Hizukuri et al., 1983; Hizukuri, 1996). It was also shown that amylose chains of DP 10-13 exhibit A-type crystals, while those of DP ≥ 14 yield B- or C-type crystals (Gidley and Bulpin, 1987; Pfannemüller, 1987). The ratio of number of chains DP10-13/number of chains of 13-18 was calculated to be approximately 1.59 and 1.30 in possible A-chains from Kinmaze and IR36, respectively, whereas that was approximately 0.97 and 0.87 in those from EM10 and IR36*ae*, respectively (Fig. 8), consistent with results reported previously cited above. In summary, it was confirmed that the length of external segments of chains of amylopectin is a determinant of the crystalline allomorph of starch granules.

Based on the present results, firstly, the average length of external segments of cluster chains with DP up to approximately 24 greatly affects the type of crystalline allomorph of starch granules. Secondly, it can be also pointed out that the presence of second branches in the cluster synthesized by BEIIb would play an important role in the crystallization of amylopectin double helices in the A-type crystal. Currently, it is well known that *ae* starch is highly resistant to thermal gelatinization and hydrolysis by hydrolytic enzymes compared to other starches (Tsuiki et al., 2018; Wang et al., 2017; Nakamura, 2018), and therefore a better understanding of the relationship between structures and functional properties of starches having various structures will be important for the use of starch for food and industrial applications.

5 CONCLUSION

The present study aimed to examine the structural features of A-type or B-type amylopectin which are responsible for the A-type or B-type crystals, respectively, of starch granules by using starches in *japonica* and *indica* rice wild-type varieties and their *be2b* (*ae*) mutants, because it is known that any wild-type varieties of cereals so far examined have A-type starch crystals in their endosperm whereas their *be2b* (*ae)* mutants produce B-type starch crystals (Hizukuri, 1996; Shannon et al., 2009). The present comparative studies with starches from both *japonica*-type and *indica*-type rice wild-type varieties and their *be2b* mutants could provide us with useful criteria to distinguish A-type amylopectin from B-type amylopectin, because it is widely known that the fine structure of amylopectin in starch from *japonica*- and *indica*-type rice endosperm greatly differs from each other (Umemoto et al., 1999; Nakamura et al., 2002, 2005). Analysis of the chain-length distribution of component chains of amylopectin and their Φ-LD (internal chains) indicated that the average length of cluster chains (A and B1 chains) of amylopectin was clearly longer in B-type amylopectin found in both *be2b* mutants than that in A-type amylopectin formed in their wild-types (Figs. 1-4 and Supplementary Table S1). The results can be explained by a specific role of BEIIb in the formation of the second branches inside the cluster. In the *be2b* mutants the second branches were deficient in the amylopectin cluster, and thus the average length of cluster chains became longer than that in wild-types (Fig. 5). On the other hand, although chain-length of cluster chains in IR36 amylopectin was apparently longer than that in Kinmaze amylopectin (Fig. 2B), both amylopectins were considered to have the second branches formed by BEIIb as well as the first branches formed mainly by BEI, as presented by Figs. 5A and 5B. The present study strongly suggests that the second branches synthesized by BEIIb would play an important role in allying double helices of amylopectin in compact and regular manner, and this results in the crystallization of amylopectin chains in the A-type allomorph. This study claims that not only the average chain-length of cluster chains but also the presence of the second branches in the cluster are important for the A-type crystalline allomorph of starch granules.

ACKNOWLEDGEMENTS

We thank Dr. Hikaru Satoh for providing us with EM10 as the experimental material. We also Dr. Naoko Fujita for help to use facilities in Akita Prefectural University. This study was funded by JSPS KAKENHI Grant Number JP19H05721 (GMa).

REFERENCES

Buléon, A., Colonna, P., Plachot, V., & Ball, S. (1998). Starch granules: Structure and biosynthesis. *International Journal of Biological Macromolecules, 23,* 85-112.

Butardo, V.M., Fitzgerald, M.A., Bird, A.R., Gidley, M.J., Flanagan, B.M., Larroque, O., Resurreccion, A.P., Laidlaw, H.K.C., Jobling, S.A., Morell, M.K. & Rahman, S. (2011). Impact of down-regulation of starch branching enzyme IIb in rice by artificial microRNA- and hairpin RNA-mediated RNA silencing. *Journal of Experimental Botany, 62,* 4927-4941.

French, D. (1972). Fine structure of starch and its relationship to the organization of starch granules. *Journal of Japanese Society of Starch Science, 19,* 8-25.

French, D. (1984). Organization of starch granules, In R.L. Whistler, J.N. BeMiller, and E. Paschall (Eds.), *Starch: Chemistry and Technology, second ed.* (pp. 183-247). San Diego, New York, Boston, London, Sydney, Tokyo, and Toronto: Academic Press.

Gérard, C., Planchot, V., Colonna, P. & Bertoft, E. (2000). Relationship between branching density and crystalline structure of A- and B-type maize mutant starches. *Carbohydrate Research, 326,* 130-144.

Gidley, M.J. & Bulpin, P.V. (1987). Crystallization of malto-oligosaccharides at models of the crystalline forms of starch. *Carbohydrate Research, 161,* 291-300.

Hieu, H.C., Li, H., Miyauchi, Y., Mizutani, G., Fujita, N. & Nakamura, Y. (2015). Wetting effect on optical sum frequency generation (SFG) spectra of D-glucose, D-fructose, and sucrose. *Spectrochimica Acta A138,* 834-839.

Hizukuri, S. (1986). Polymodal distribution of the chain lengths of amylopectin, and its significance. *Carbohydrate Research, 147,* 342-347.

Hizukuri, S. (1996). Starch: Analytical aspects. In A.-C. Eliasson (Ed.), *Carbohydrates in Food* (pp. 347-429). Marcel Dekker, Inc.: New York, Basel, and Hong Kong.

Hizukuri, S., Kaneko, T. & Takeda, Y. (1983). *Biochimica Biophysica Acta, 760,* 188-191.

Imberty, A., Buléon, A., Tran, V. & Pérez, S. (1991). Recent advances in knowledge of starch structure. *Starch/Stärke, 43,* 375-384.

Jane, J.L., Wong, K.S. & McPherson, A.E. (1997). Branch-structure difference in starches of A- and B-type X-ray patterns revealed by their Naegeli dextrins. *Carbohydrate Research, 300,* 219-227.

Kainuma, K. & French, D. (1972). Naegeli amylodextrin and its relationship to starch granule structure. II. Role of water in crystallization of B-starch. *Biopolymers, 11,* 2241-2250.

Kong, L., Lee, C., Kim, S.H. & Ziegler, G.R. (2014). Characterization of starch polymorphic structures using vibrational sum frequency generation spectroscopy. *Journal of Physical Chemistry. B 118,* 1775-1783.

Kouyama, W., Nishida, T., Hien, K.T.T., Mizutani, G., Hasegawa, H. & Miyamura, H. (2016). Optical sum frequency generation spectroscopy of cracked non-glutinous rice (*Oryza sativa* L.) kernels. *Journal of Biomaterial Nanobiotechnology, 7,* 13-18.

Miyauchi, Y., Sano, H. & Mizutani, G. (2006). Selective observation of starch in a water plant using optical sum-frequency microscopy. *Journal of Optical Society of America. A 23,* 1687-1690.

Nagasaki, A., Matsuba, G., Ikemoto, Y., Moriwaki, T., Ohta, N. & Osaki, K. (2021). Analysis of the sol and gel structures of potato starch over a wide spatial scale. *Food Science and Nutrition, 9,* 4916-4926.

Nakamura, Y. (2002). Towards a better understanding of the metabolic system for amylopectin biosynthesis in plants: Rice endosperm as a model tissue. *Plant & Cell Physiology, 43,* 718-725.

Nakamura, Y. (2015). Biosynthesis of reserve starch. In Y. Nakamura (Ed.), *Starch: Metabolism and Structure* (pp. 161-209). Springer: Tokyo, Heidelberg, New York, Dordrecht, London.

Nakamura, Y. (2018). Rice starch biotechnology: Rice endosperm as a model of cereal endosperms. *Starch/Stärke, 70,* 1600375.

Nakamura, Y., Sakurai, A., Inaba, Y., Kimura, K., Iwasawa, N. & Nagamine, T. (2002). The fine structure of amylopectin in endosperm from Asian cultivated rice can be largely classified into two classes. *Starch/Stärke, 54,* 117-131.

Nakamura, Y., Francisco, Jr. P.B., Hosaka, Y., Sato, A., Sawada, T., Kubo, A. & Fujita, N. (2005). Essential amino acids of starch synthase IIa differentiate amylopectin structure and starch quality between *japonica* and *indica* rice varieties. *Plant Molecular Biology, 58,* 213-227.

Nakamura, Y., Ono, M., Hatta, T., Kainuma, K., Yashiro, K., Matsuba, G., Matsubara, A., Miyazato, A. & Mizutani, G. (2020). Effects of BEIIb-deficiency on the cluster

500 structure of amylopectin and the internal structure of starch granules in endosperm and
501 culm of *japonica*-type rice. *Frontiers in Plant Science, 11,* 571346.
502 Nakamura, Y. & Kainuma, K. (2022). On the cluster structure of amylopectin. *Plant*
503 *Molecular Biology, 108,* 291-306.
504 Nakamura,Y., Kubo, A., Ono, M., Yashiro, K., Matsuba, G., Wang, Y., Matsubara, A.,
505 Mizutani, G., Matsuki, J. & Kainuma, K. (2022). Changes in fine structure of
506 amylopectin and internal structures of starch granules in developing endosperms and
507 culms caused by starch branching enzyme mutations of *japonica* rice. *Plant Molecular*
508 *Biology, 108,* 481-496.
509 Nishi, A., Nakamura, Y., Tanaka, N. & Satoh, H. (2001). Biochemical and genetic analysis
510 of the effects of *amylose-extender* mutation in rice endosperm. *Plant Physiology, 127,*
511 459-472.
512 Ohdan, T., Francisco, Jr. P.B., Sawada, T., Hirose, T., Terao, T., Satoh, H. & Nakamura,
513 Y. (2005). Expression profiling of genes involved in starch synthesis in sink and source
514 organs of rice. *Journal of Experimental Botany, 56,* 3229-3244.
515 O'Shea, M.G., Samuel, M.S., Konik, C.M. & Morell, M.K. (1998). Fluorophore-assisted
516 carbohydrate electrophoresis (FACE) of oligosaccharides: Efficiency of labeling and
517 high-resolution separation. *Carbohydrate Research, 307,* 1-12.
518 Peat, S., Whelan, W.J. & Thomas, G.J. (1952). Evidence of multiple branching in waxy
519 maize starch. *Journal of Chemical Society,* 4546-4548.
520 Pfannemüller, B. (1987). *International Journal of Biological Macromolecules, 9,* 105-
521 108.
522 Sawada, T., Nakamura, Y., Ohdan, T., Saitoh, A., Francisco, Jr., P.B., Suzuki, E., Fujita,
523 N., Shimonaga, T., Fujiwara, S., Tsuzuki, M., Colleoni, C. & Ball, S. (2014). Diversity
524 of reaction characteristics of glucan branching enzymes and the fine structure of α-
525 glucan from various sources. *Archives of Biochemistry and Biophysics, 562,* 9-21.
526 Shannon, J.C., Garwood, D.L. & Boyer, C.D. (2009). Genetics and physiology of starch
527 development. In J. BeMiller and R. Whistler (Eds.), *Starch, Chemistry and Technology,*
528 *3rd ed.* (pp. 23-82). Academic Press: New York.
529 Tanaka, N., Fujita, N., Nishi, A., Satoh, H., Hosaka, Y., Ugaki, M., Kawasaki, S. &
530 Nakamura, Y. (2004). The structure of starch can be manipulated by changing the
531 expression levels of starch branching enzyme IIb in rice endosperm. *Plant*
532 *Biotechnology Journal, 2,* 507–516.
533 Tsuiki, K., Fujisawa, H., Itoh, A., Sato, M. & Fujita, N. (2016). Alterations of starch
534 structure lead to increased resistant starch of steamed rice: Identification of high
535 resistant starch line lines. *Journal of Cereal Science, 68,* 88-92.

Umemoto, T., Nakamura, Y., Satoh, H. & Terashima, K. (1999). Differences in amylopectin structure between two rice varieties in relation to the effects of temperature during grain-filling. *Starch/Stärke, 51,* 58-62.

Umemoto, T., Yano, M., Satoh, H., Shomura, A. & Nakamura, Y. (2002). Mapping of a gene responsible for the difference in amylopectin structure between *japonica*-type and *indica*-type rice varieties. *Theoretical Applied Genetics, 104,* 1-8.

Waigh, T.A., Gidley, M.J., Komanshek, B. & Donald, A.M. (2000). The phase transformations in starch during gelatinization: a liquid crystalline approach. *Carbohydrate Research, 328,* 165-176.

Wang, J., Hu, P., Chen, Z., Liu, Q. & Wei, C. (2017). Progress in high-amylose cereal crops through inactivation of starch branching enzyme. *Frontiers in Plant Science, 8,* 469.

Wei, C., Xu, B., Qin, F., Yu, H., Chen, C., Meng, X., Zhu, L., Wang, Y., Gu, M. & Liu, Q. (2010). C-type starch from high-amylose rice resistant starch granules modified by antisense RNA inhibition of starch branching enzyme. *Agricultural Food Chemistry, 58,* 7383-7388.

Yamaguchi, M., Kainuma, K. & French, D. (1979). Electron microscopic observations of waxy maize starch. *Journal of Ultrastructural Research, 69,* 249-261.

Yano, M., Okuno, K., Kawakami, J., Satoh, H. & Omura, T. (1985). High amylose mutants of rice, *Oryza sativa* L. *Theoretical Applied Genetics, 69,* 253-257.

Ying, Y., Zhang, Z., Tappiban, P., Xu, F., Deng, G., Dai, G. & Bao, J.S. (2022). Starch fine structure and functional properties during seed development in BEIIb active and deficient rice. *Carbohydrate Polymers, 292,* 119640.

Zhang, Z., Hu, Y., Zhao, J., Zhang, Y., Ying, Y., Xu, F. & Bao, J.S. (2022). The role of different *Wx* and *BEIIb* allele combinations on fine structures and functional properties of *indica* rice starches. *Carbohydrate Polymers, 278,* 118972.

SUPPORTING INFORMATION

Additional supporting information can be found online in the Supporting Information section at the end of this article.

Legends for figures

Fig. 1 Chain-length distribution of amylopectin in mature endosperms of a wild-type *japonica* cultivar Kinmaze, a wild-type *indica* cultivar IR36, and their *be2b* mutant lines, EM10 and IR36ae, respectively. The vertical axis presents the proportion (molar %) of the amount of each chain to the total amounts of chains with degree of polymerization (DP) from 6 to 90, whereas the horizontal axis shows the DP value of the chain. Amylopectin of Kinmaze (A), IR36 (B), EM10 (C), and IR36*ae* (D). The experiments were repeated at least three times until all these results were consistent, whereas each figure shows one representative result. Values are the averages calculated from three replicate measurements. Standard deviations were too small to be shown in the figure.

Fig. 2 Difference in amylopectin between EM10 and Kinmaze, calculated from data of EM10 subtracted by those of Kinmaze. A, Difference in amylopectin between EM10 and Kinmaze, calculated from data of EM10 subtracted by those of Kinmaze. B, Difference in amylopectin between Kinmaze and IR36, calculated from data of Kinmaze subtracted by those of IR36. C, Difference in amylopectin between IR36*ae* and IR36, calculated from data of IR36*ae* subtracted by those of IR36. D, Difference in amylopectin between EM10 and IR36*ae*, calculated from data of EM10 subtracted by those of IR36*ae*. The other conditions are the same as in Fig. 1.

Fig. 3 Chain-length distribution of phosphorylase-limit dextrins (Φ-LD) of amylopectin in mature endosperms of a wild-type *japonica* cultivar Kinmaze, a wild-type *indica* cultivar IR36, and their *be2b* mutant lines, EM10 and IR36*ae*, respectively. Φ-LD of Kinmaze (A), IR36 (B), EM10 (C), and IR36*ae* (D). The other conditions are the same as in Fig. 1, except that data were obtained for chains with degree of polymerization (DP) from 4 to 60.

Fig. 4 Comparison of chain-length distribution of Φ-LD of amylopectin in mature endosperms of a wild-type *japonica* cultivar Kinmaze, its *be2b* mutant line, EM10, a wild-type *indica* cultivar IR36, and its *be2b* mutant line, IR36*ae*. A, Difference in Φ-LD between EM10 and Kinmaze, calculated from data of EM10 subtracted by those of Kinmaze. B, Difference in Φ-LD between Kinmaze and IR36, calculated from data of

609 Kinmaze subtracted by those of IR36. C, Difference in Φ-LD between EM10 and IR36*ae*,
610 calculated from data of EM10 subtracted by those of IR36*ae*. The other conditions are the
611 same as in Fig. 3.
612
613
614 **Fig. 5** A schematic representation of the hypothetical cluster structure of amylopectin in
615 endosperm from a wild-type *japonica* cultivar Kinmaze (A), a wild-type *indica* cultivar
616 IR36 (B), and their *be2b* mutant lines, EM10 (C) and IR36*ae* (D), respectively.
617
618
619 **Fig. 6** Wide angle X-ray scattering (WAXS) analysis of starch granules in mature
620 endosperms from a wild-type *japonica* cultivar Kinmaze (A), a wild-type *indica* cultivar
621 IR36 (B), and their *be2b* mutant lines, EM10 (C) and IR36*ae* (D), respectively. See
622 **Materials and methods** in details.
623
624
625 **Fig. 7** SFG spectra of starch granules in mature endosperms from a wild-type *japonica*
626 cultivar Kinmaze (A), a wild-type *indica* cultivar IR36 (B), and their *be2b* mutant lines,
627 EM10 (C) and IR36*ae* (D), respectively. See **Materials and methods** in details.
628
629
630 **Fig. 8** The hypothetical chain-length distribution of A chains in a wild-type *japonica*
631 cultivar Kinmaze (A), a wild-type *indica* cultivar IR36 (B), and their *be2b* mutant lines,
632 EM10 (C) and IR36*ae* (D), respectively. The chain-length distribution of hypothetical A
633 chains in the DP range of 6-18 were obtained by the difference of chain-length distribution
634 between native amylopectin (DP 6-60) and its Φ-LD (DP ≥ 5), although each DP of Φ-
635 LD was added by DP12. See text in details.
636
637
638

Fig. 1

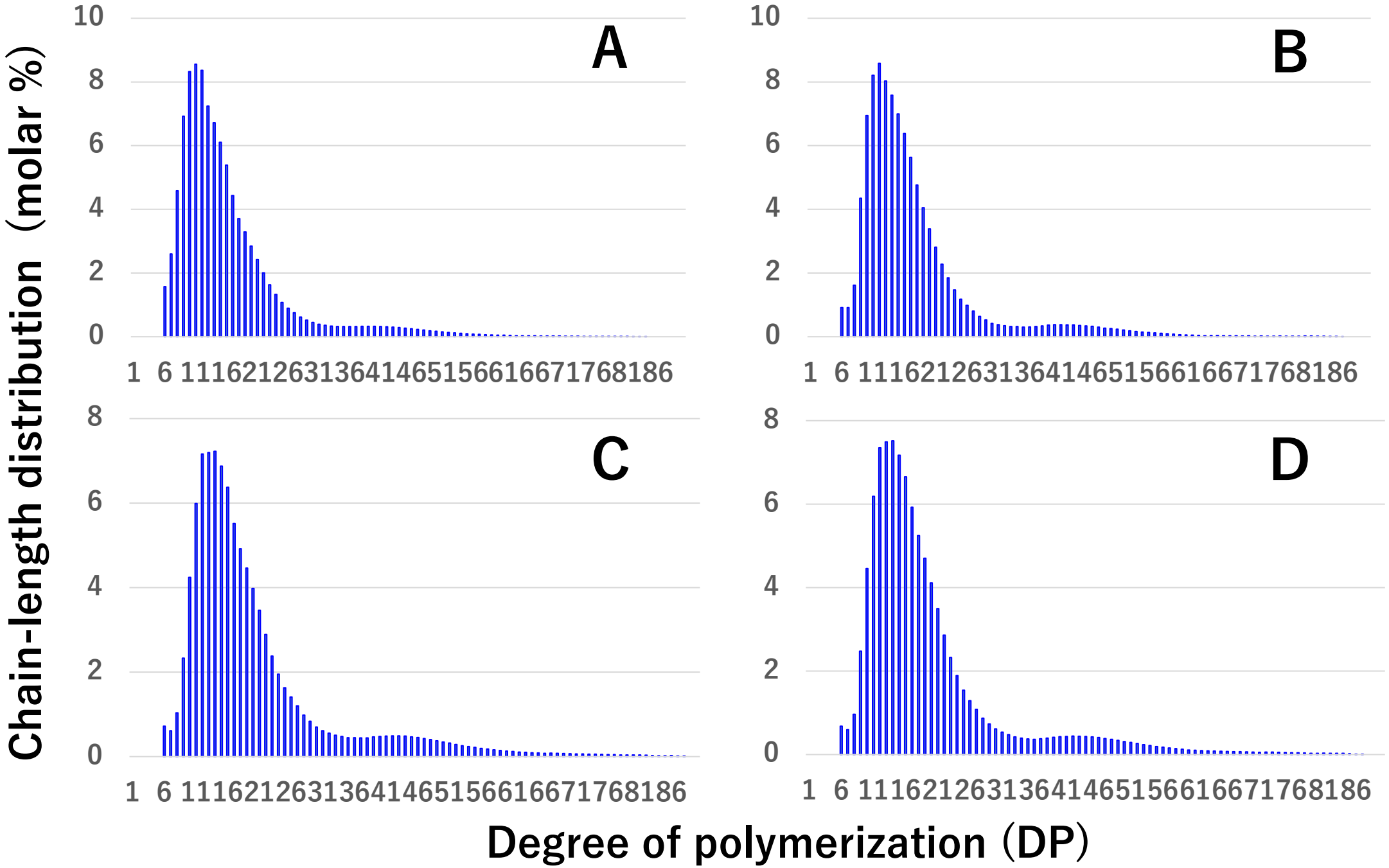
A
B
C
D
10
8
6
4
2
0
1 6 11 16 21 26 31 36 41 46 51 56 61 66 71 76 81 86
Chain-length distribution (molar %)
Degree of polymerization (DP)

Fig. 2

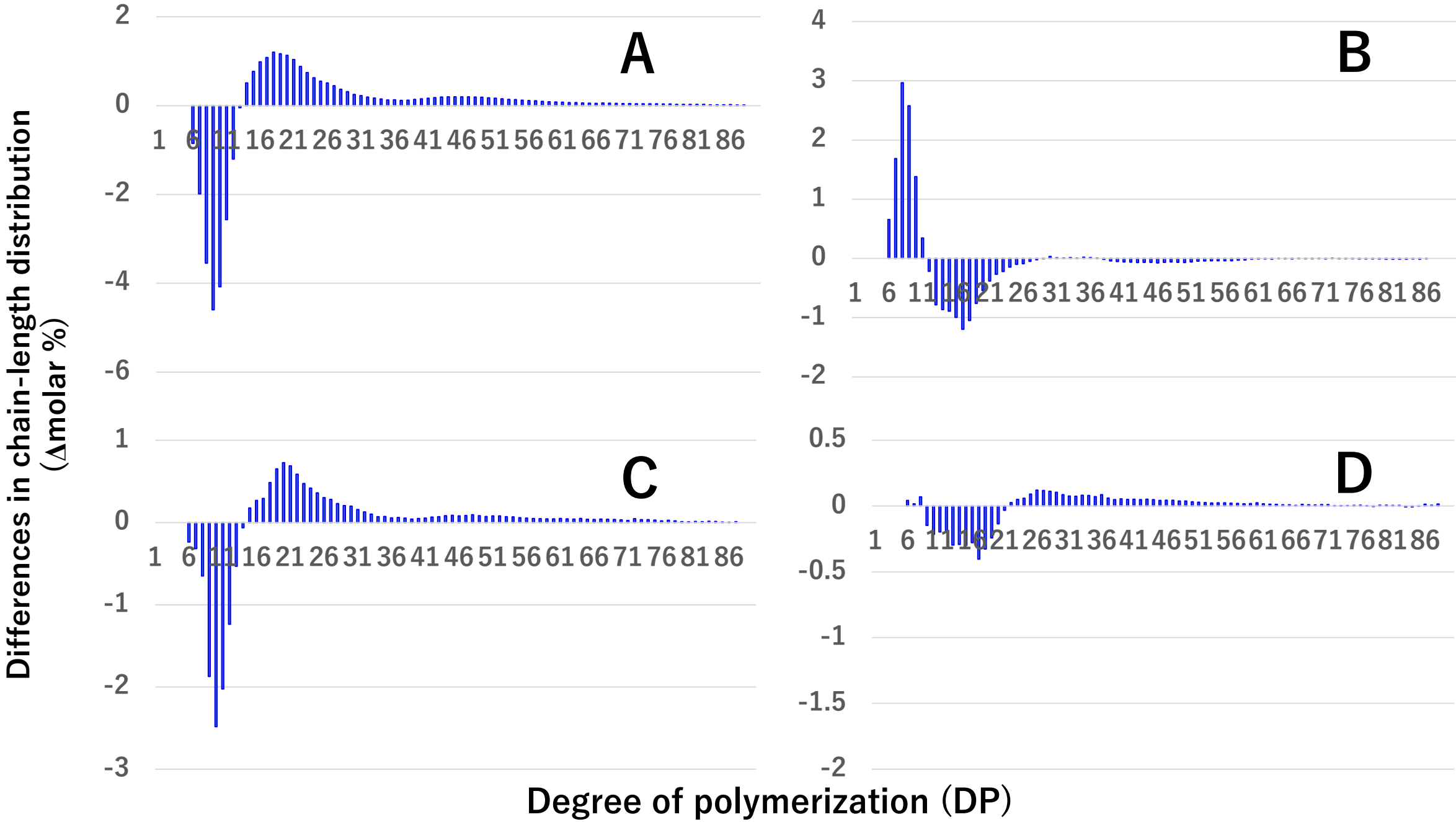
A
B
C
D
Differences in chain-length distribution (Δmolar %)
Degree of polymerization (DP)

Fig. 3

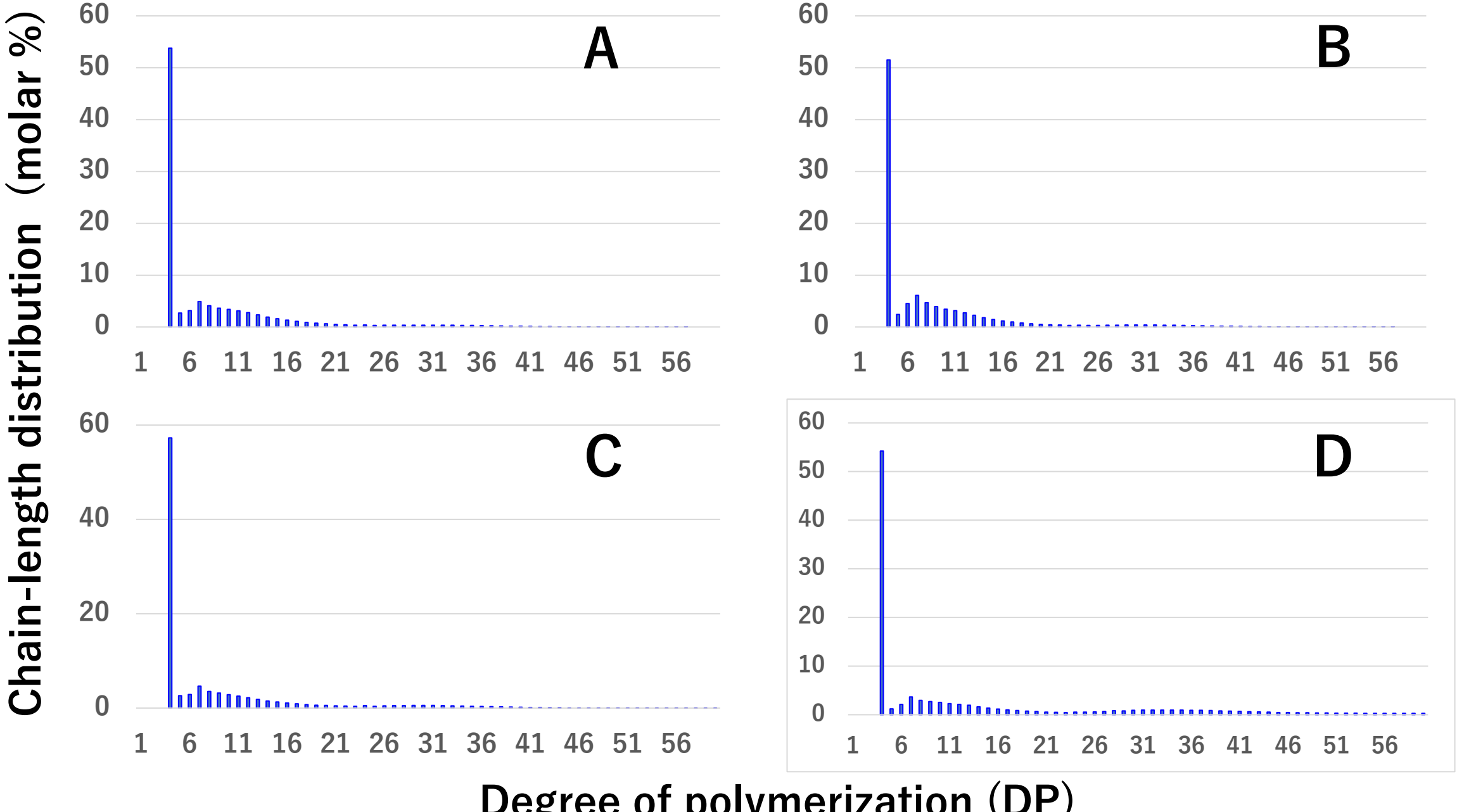
Chain-length distribution (molar %)
A
B
C
D
60
50
40
30
20
10
0
1 6 11 16 21 26 31 36 41 46 51 56
Degree of polymerization (DP)

Fig. 4

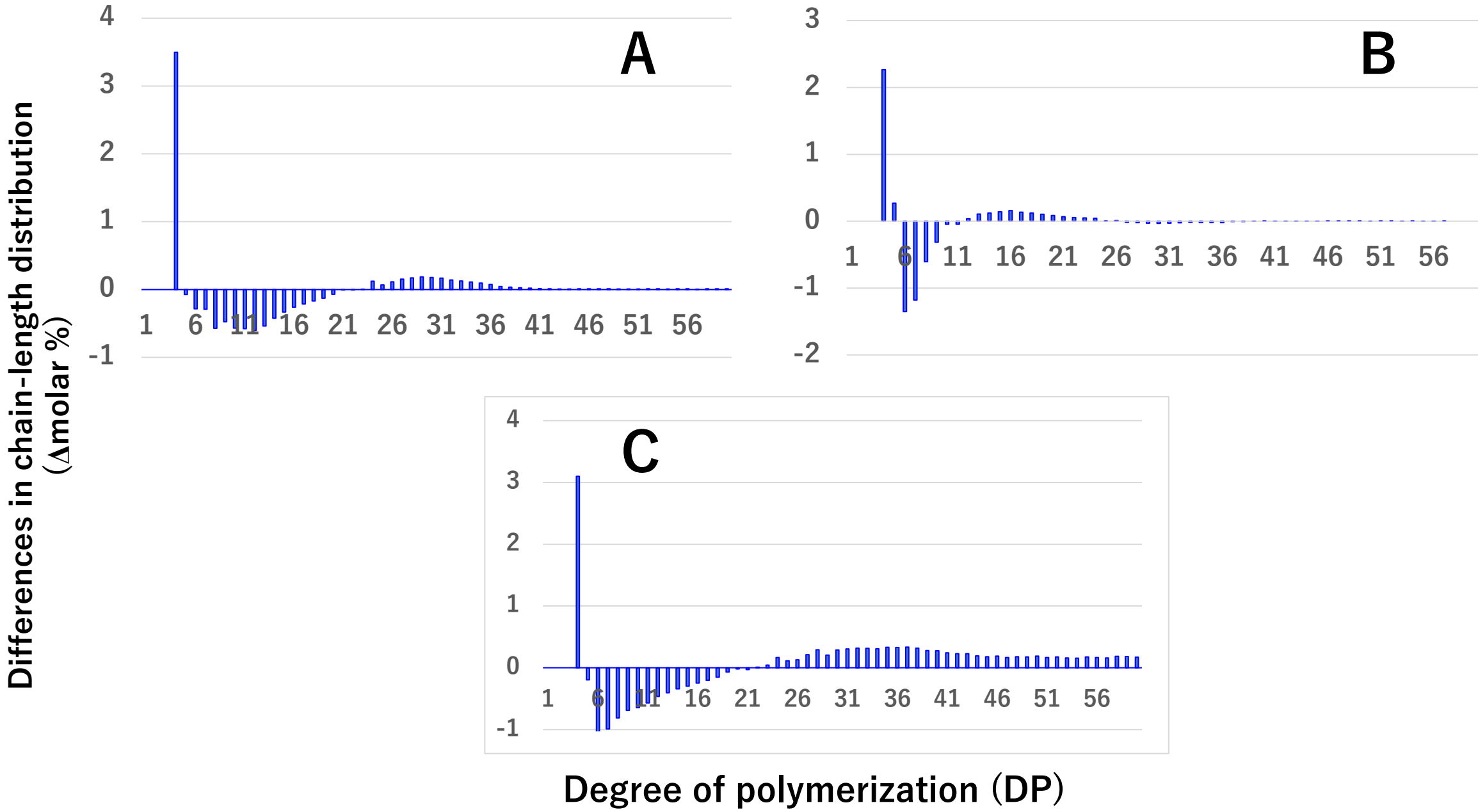
A
B
C
Differences in chain-length distribution
(Δmolar %)
Degree of polymerization (DP)
4
3
2
1
0
-1
-2
1
6
11
16
21
26
31
36
41
46
51
56

Fig. 5

(A)

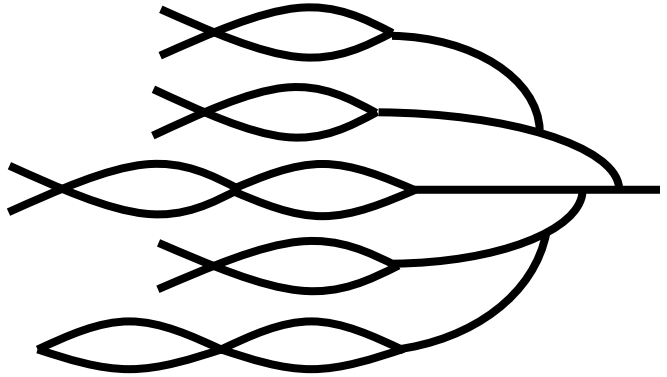

Kinmaze (*japonica*)

(B)

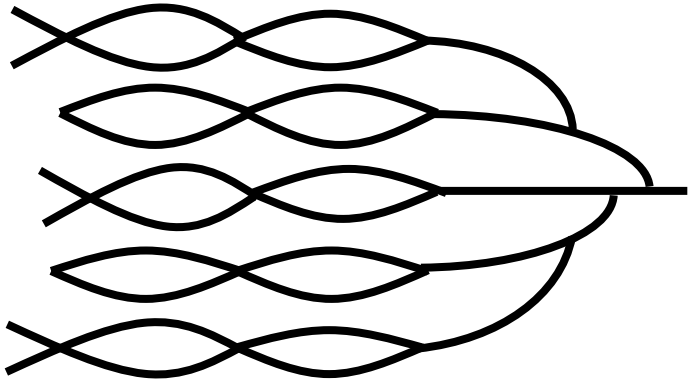

IR36 (*indica*)

(C)

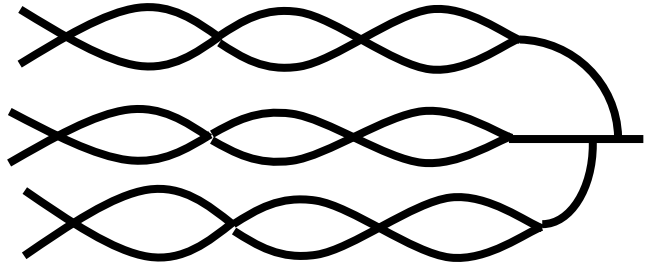

EM10

(D)

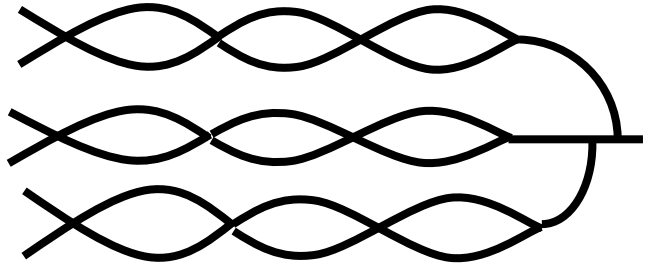

IR36ae

Fig. 6

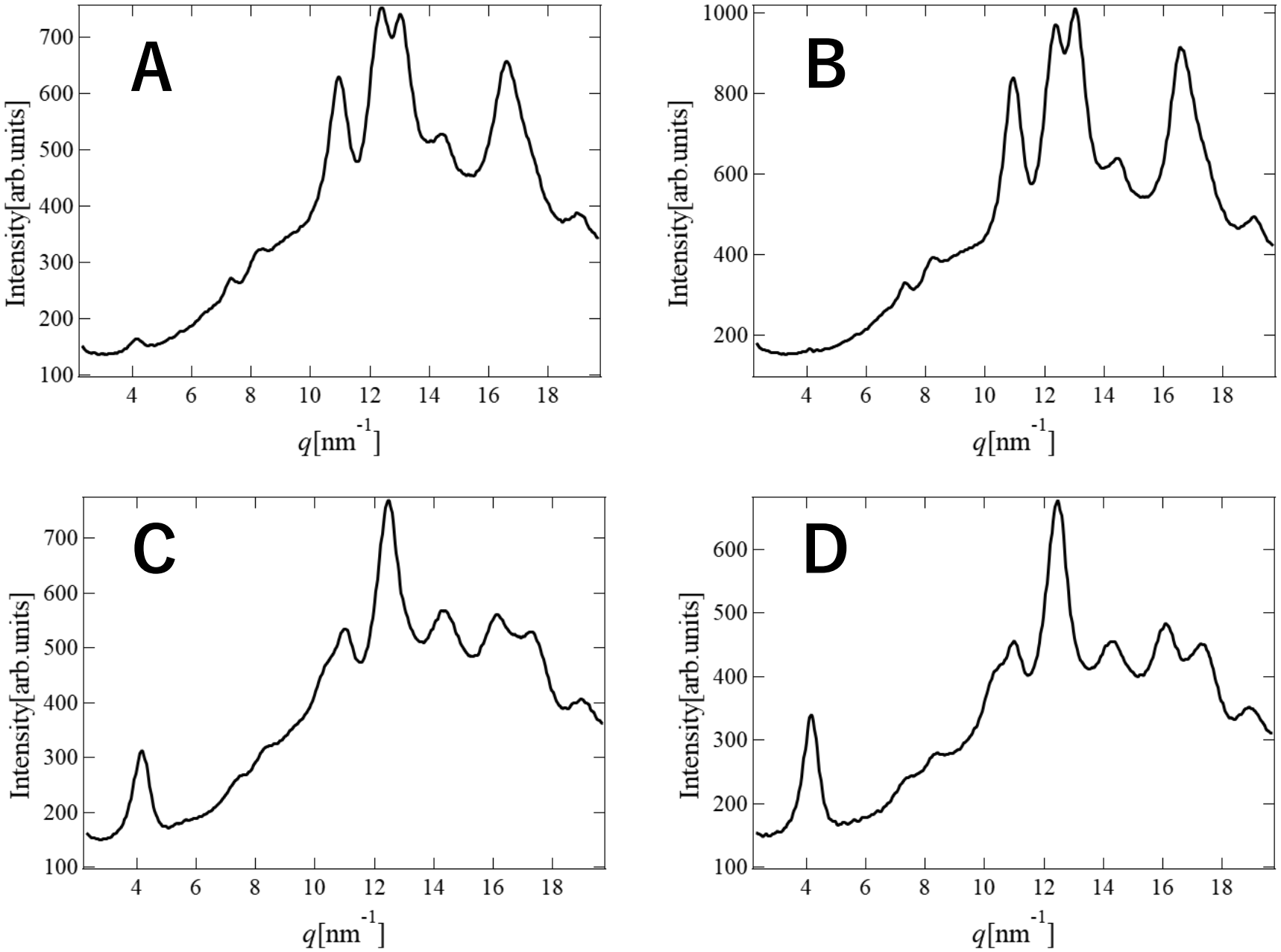

Fig. 7

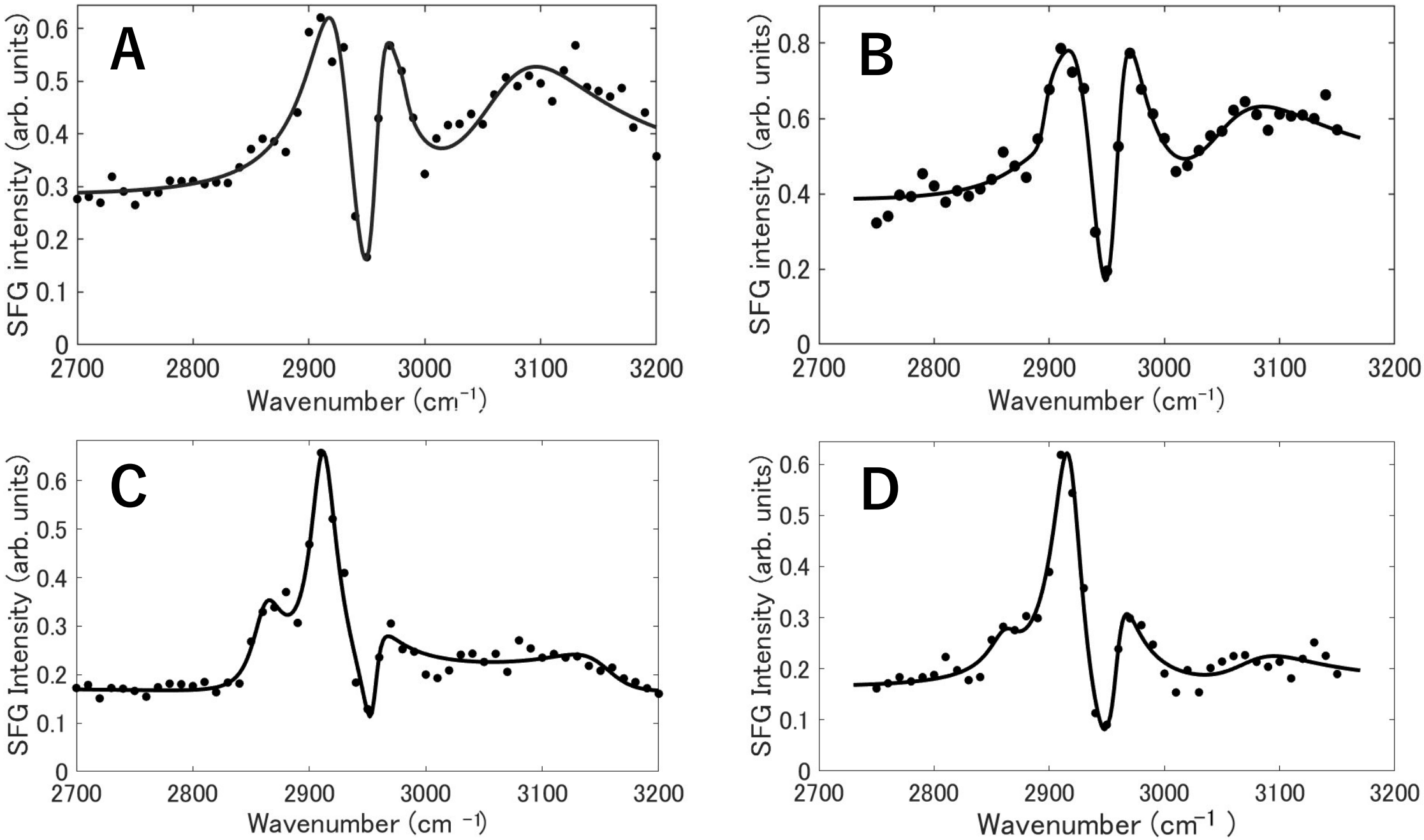
A
B
C
D
SFG intensity (arb. units)
SFG Intensity (arb. units)
Wavenumber (cm^{-1})
2700
2800
2900
3000
3100
3200

Fig. 8

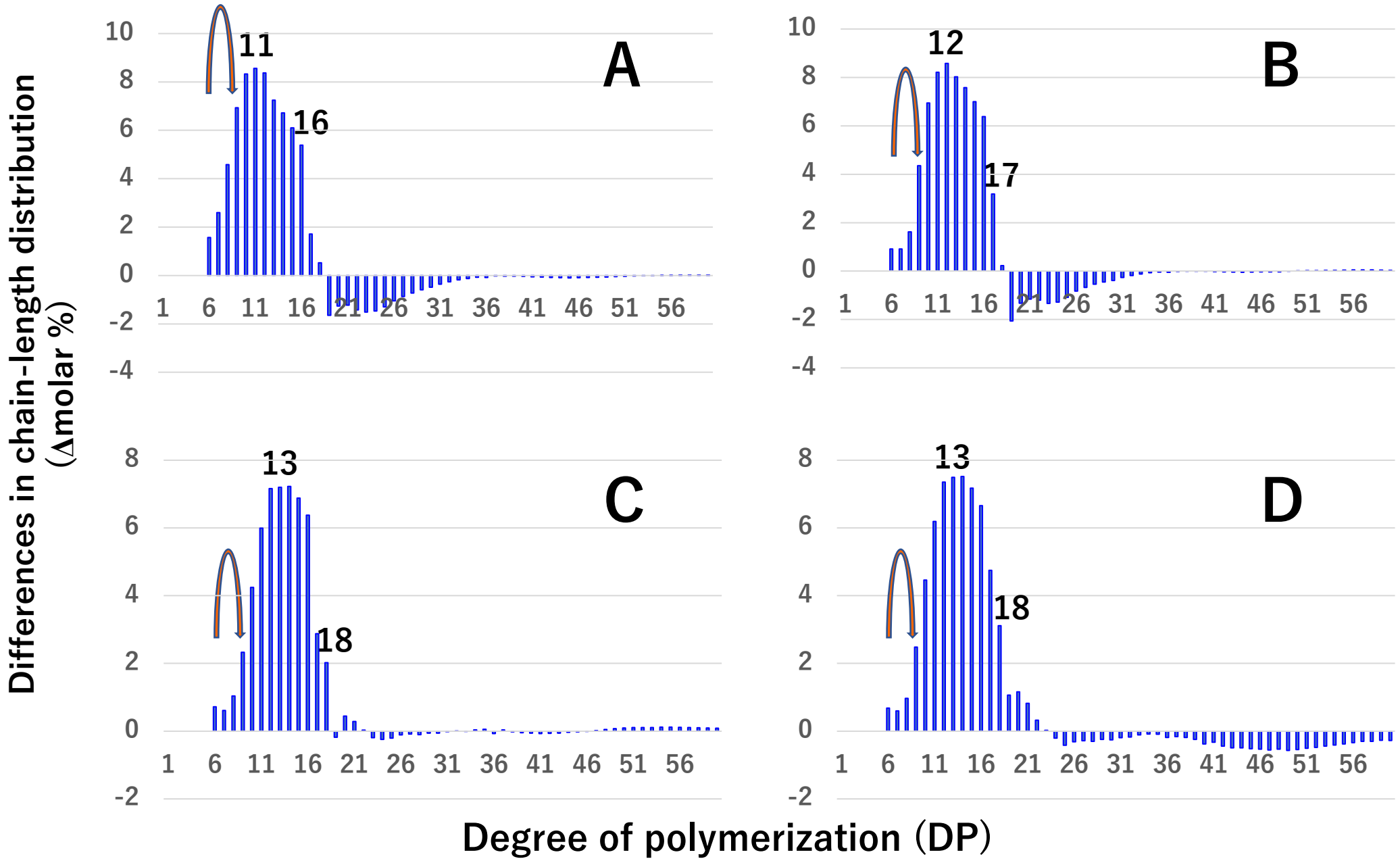
Differences in chain-length distribution
(Δmolar %)
A
11
16
B
12
17
C
13
18
D
13
18
Degree of polymerization (DP)